

1 **Above- and below-ground biodiversity responses to the prolonged flood pulse in central-**  
2 **western Amazonia, Brazil.**

3 Yennie K. Bredin<sup>1§\*</sup>, Laura L. Hess<sup>2</sup>, Andressa B. Scabin<sup>3</sup>, Micah Dunthorn<sup>4,5,6</sup>, Torbjørn  
4 Haugaasen<sup>1</sup>, Carlos A. Peres<sup>3,7</sup>, Henrik R. Nilsson<sup>8</sup>, Alexandre Antonelli<sup>8,9,10</sup>, Camila D.  
5 Ritter<sup>5,11§\*</sup>

6 <sup>1</sup>Faculty of Environmental Sciences and Natural Resource Management, Norwegian University  
7 of Life Sciences, Ås, Norway.

8 <sup>2</sup> Earth Research Institute, University of California Santa Barbara, Santa Barbara, United States  
9 of America.

10 <sup>3</sup>Instituto Juruá, Manaus, AM, Brazil.

11 <sup>4</sup>Natural History Museum, University of Oslo, Oslo, Norway.

12 <sup>5</sup>Eukaryotic Microbiology, University of Duisburg-Essen, Essen, Germany.

13 <sup>6</sup>Centre for Water and Environmental Research (ZWU), University of Duisburg-Essen, Essen,  
14 Germany.

15 <sup>7</sup> School of Environmental Sciences, University of East Anglia, Norwich NR4 7TJ, Norwich,  
16 United Kingdom.

17 <sup>8</sup>Gothenburg Global Biodiversity Centre, Department of Biological and Environmental Sciences,  
18 University of Gothenburg, Gothenburg, Sweden.

19 <sup>9</sup>Department of Plant Sciences, University of Oxford, Oxford, United Kingdom

20 <sup>10</sup>Royal Botanic Gardens, Kew, Richmond, United Kingdom.

21 <sup>11</sup>Grupo Integrado de Aquicultura e Estudos Ambientais, Departamento de Zootecnia,  
22 Universidade Federal do Paraná, Rua dos Funcionários, 1540, Juvevê, 80035-050 Curitiba, PR,  
23 Brazil.

24

25 \*Corresponding authors: Yennie K. Bredin, [yennie.bredin@nmbu.no](mailto:yennie.bredin@nmbu.no); Camila D. Ritter,

26 [kmicaduarte@gmail.com](mailto:kmicaduarte@gmail.com).

27 §Both authors have contributed equally to this work.

28

29 **Abstract**

30 Amazonia encompasses forests that grow in areas that are periodically inundated by overflowing  
31 rivers. The inundation depth and duration vary according to the slope of the terrain, creating a  
32 flooding gradient. This gradient directly affects the biota, but the effect on soil organisms  
33 remains elusive. Here, we use DNA metabarcoding to estimate prokaryote and eukaryote  
34 diversity from soil and litter samples in a seasonally flooded forest and its adjacent unflooded  
35 forest in central-western Amazonia using 16S and 18S gene sequences, respectively. We  
36 characterize the below-ground diversity and community composition based on Amplicon  
37 Sequence Variants (ASVs) along the flooding gradient. We test for the relationship of soil biota  
38 with the flooding gradient, soil properties and above-ground woody plant diversity. The flooding  
39 gradient did not explain below-ground biodiversity. Nor was the below-ground diversity  
40 explained by the above-ground woody plant diversity. However, we found taxonomic groups not  
41 previously reported in Amazonian seasonally flooded forests. Also, the flooding gradient and  
42 woody plant diversity did, in part, explain the community composition of soil bacteria. Although  
43 the effects of the flooding gradient, soil properties and above-ground woody plant diversity is  
44 hard to quantify, our results thus indicate that flood stress could influence below-ground bacterial  
45 community composition.

46 **Keywords:** Amazonia; Below-ground biodiversity; Juruá; Metabarcoding; Seasonally flooded  
47 forests; Flooding gradient.

## 48 **1. Introduction**

49 Amazonia comprises the largest continuous tropical rainforest in the world. Accounting for only  
50 3.6% of the terrestrial global surface, Amazonia harbours 10% of the world's known biodiversity  
51 (Maretti, 2014) and potentially hosts the largest Linnaean biodiversity knowledge deficit on  
52 Earth (Moura and Jetz, 2021). Amazonia is heterogeneous and encompasses several distinct  
53 environments. These include tropical rainforests known as terra firme, non-forested areas, such  
54 as the edaphic open areas associated with white sand soils, and seasonally flooded forests  
55 (Myster, 2016). Seasonally flooded forests grow in areas that are periodically inundated by  
56 overflowing rivers, lakes and perennial streams (Prance, 1996). These forests are characterized  
57 by low taxonomic diversity compared to terra firme forests (Haugaasen and Peres, 2006; Myster,  
58 2016; ter Steege and Hammond, 2001). However, they have a characteristic fauna and flora often  
59 restricted to these environments (Myster, 2016; Ramalho et al., 2016). At least 9% of the  
60 Amazon basin is formed by seasonally or permanently flooded forests (Hess et al., 2015), which  
61 are crucial for the maintenance of biodiversity and climatic dynamics in the region (Castello and  
62 Macedo, 2016).

63 Two determinants are decisive for the extent of periodically flooded forests in Amazonia. The  
64 first is the uneven annual distribution of rainfall. In most parts of Amazonia, the rainy season is  
65 followed by a drier period lasting several months, but this is not synchronous across the basin.  
66 The second is the topography of the Amazon basin and its low-lying floodplains. Combined,  
67 these factors lead to an annual rise in fluvial discharge which causes an enormous flood pulse  
68 (Junk, 1989; Kubitzki, 1990) and gives rise to an aquatic and a terrestrial phase in the flooded  
69 areas. The inundation depth and duration of the flood waters vary according to the slope of the  
70 terrain and the volume of the rivers that flood the landscape (Assis et al., 2015; Wittmann et al.,

71 2010). This creates a gradient in flood depth and duration from low-lying areas flood to greater  
72 depths for longer periods of time to areas higher up in the terrain that flood for shorter periods.  
73 This gradient directly affects the biota, generating thresholds for species establishment (Petit and  
74 Hampe, 2006). Additionally, the physical and chemical properties of the waters also affect the  
75 distribution of biota in inundated areas (Prance, 1979).

76 In the Amazon basin, seasonally flooded forests can be classified into two major types according  
77 to the hydro-chemical characteristics of the rivers that flood them (Assis et al., 2015; Haugaasen  
78 and Peres, 2006; Myster, 2016; Prance, 1979). Whereas eutrophic várzea forests are flooded by  
79 nutrient-rich white-water rivers originating in the Andes, oligotrophic igapó forests are inundated  
80 by nutrient poor, black- or clear-water rivers (Ríos-Villamizar et al., 2020). Thus, fluvial  
81 geochemistry determines the physical properties of substrate, such as moisture retention and  
82 hydraulic conductivity, accumulation of organic matter, nutrient availability and soil biota  
83 (Parolin et al., 2004). It has been demonstrated that changes in above-ground species richness  
84 and composition in seasonally flooded forests can occur due to the physicochemical  
85 characteristics of the water (Myster, 2016) and/or flood depth (Julião et al., 2018). Few studies  
86 have evaluated this difference in soil biota (Ritter et al., 2019b), and to our knowledge no study  
87 has yet examined the influence of the flooding gradient on seasonally flooded forest soil  
88 biodiversity.

89 Soil biota represent a large reservoir of terrestrial biodiversity and provide fundamental  
90 ecosystem services that are key to the functionality of terrestrial ecosystems (Bardgett and Van  
91 Der Putten, 2014; Pereira et al., 2018; Pietramellara et al., 2002). For instance, larger soil  
92 invertebrates are responsible for processing large amounts of detritus and make it available to  
93 other organisms (García-Palacios et al., 2013; Hättenschwiler and Gasser, 2005). Similarly,

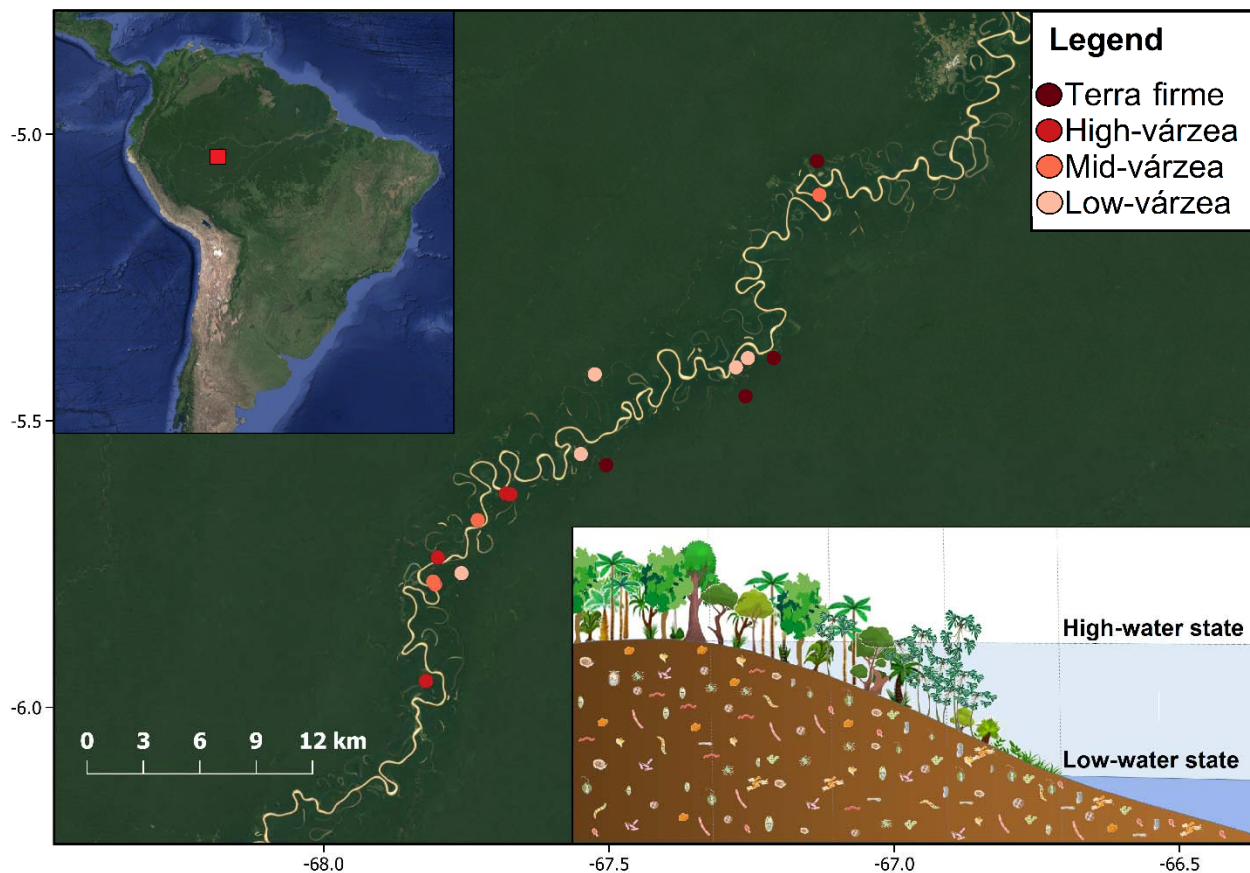
94 micro-organisms are essential for nutrient cycling (Delgado-Baquerizo et al., 2020), and  
95 ectomycorrhizal fungi underlie ecosystem processes such as soil carbon cycling (Johnson et al.,  
96 2016). Yet, soil biodiversity remains elusive and has been neglected in many global biodiversity  
97 assessments and policies (Cameron et al., 2019; Ritter et al., 2017). This omission is undoubtedly  
98 related to the scarcity of comprehensive information on soil biodiversity, especially in  
99 megadiverse and remote tropical environments, such as Amazonia. Fortunately, molecular  
100 approaches, including high throughput sequencing (HTS), such as metabarcoding (Creer et al.,  
101 2016), are now able to address many previous obstacles to understanding the diversity and  
102 composition of soil communities (Cameron et al., 2019; Ritter et al., 2019b; Tedersoo et al.,  
103 2014).

104 In this study we use a metabarcoding approach to characterize the soil biodiversity along the  
105 flooding gradient of an Amazonian várzea landscape. More specifically, we investigate the  
106 diversity and composition of soil communities across three flood-levels and explore if, and how,  
107 soil biota changes along the flooding gradient. In addition, by comparing the soil communities to  
108 the above-ground woody plant community, we examine the degree to which the above- and  
109 below-ground biodiversity are congruent. The results are discussed in relation to other studies  
110 and interpreted in light of differences experienced by seasonal flooding, soil characteristics and  
111 above-ground woody plant diversity. Finally, we draw some general implications to the  
112 conservation of Amazonian biota.

## 113 **2. Materials and Methods**

114 *2.1. Study area:* We conducted the study in the Uacari Sustainable Development Reserve  
115 (RDS Uacari) and nearby forests along the central reaches of the Juruá River, western Brazilian  
116 Amazonia (Fig. 1). The climate of the region is hot and humid with a mean annual temperature

117 of  $\sim 27^{\circ}\text{C}$ , average annual rainfall of  $\sim 3,679$  mm, and a well-defined rainy season from December  
118 until May (Hawes and Peres, 2016). We sampled above-ground woody plant communities and  
119 below-ground microbial communities at three different flood levels in várzea (VZ) and adjacent  
120 upland forest (i.e. terra firme, TF) that does not flood on a seasonal basis. This “unflooded”  
121 forest is growing on Pleistocene floodplain sediments (i.e., paleo-várzea sediments; Assis et al.,  
122 2015) abandoned by the meandering Juruá River and at higher elevations than the river’s  
123 maximum flood level. The várzea communities were sampled during the 2016 and 2017 dry  
124 seasons and the terra firme communities were sampled in the 2017 wet and dry seasons.



125  
126 **Fig. 1. Sampling localities** along the central Juruá River (main map) in the central-western  
127 Brazilian Amazon (upper left inset). The lower right inset shows a schematic cross-section of

128 flood levels in the várzea forest, with low- and high-water states separated by the dotted vertical  
129 lines. Low-várzea is low-lying and subject to the longest flooding periods (5-12 mo/yr); mid-  
130 várzea is subject to intermediate periods of flooding (2-4 mo/yr); and high-várzea is located  
131 higher up in the terrain and subject to the shortest flooding periods (0-1 mo/yr). Terra firme  
132 forests are beyond the maximum flood levels of rivers and perennial streams. Map created using  
133 QGIS3 software (Q. D. Team, 2015).

134

135 *2.2. Determination of the hydro-topographic gradient:* To position the plots along the hydro-  
136 topographic gradient, we used inundation period mapped with multi-date ALOS-1 PALSAR  
137 satellite imagery (Fine-beam mode, resampled to 30 m) freely available from the Alaska Satellite  
138 Facility Distributed Active Archive Center ([asf.alaska.edu](http://asf.alaska.edu)). Water levels at the Porto Gavião  
139 gauge on the Juruá River (66.9 W, 4.88 S) were retrieved from Brazil's Agência Nacional de  
140 Águas (ANA; <http://www.snirh.gov.br/hidroweb/serieshistoricas>) for each of the 28 PALSAR  
141 imaging dates between 2007 and 2011 (9-10 dates for each of 3 PALSAR swaths covering the  
142 forest plots). The average number of months inundated per year were calculated over the 47-year  
143 Gavião river level record (1972-2018). Due to small-scale variability in flood duration even at  
144 the 0.1 ha scale, we defined the flooding gradient by approximating the average number of  
145 months each plot was flooded annually. Thus, plots were grouped into the following four flood  
146 levels: (1) terra firme = not seasonally flooded (n = 6); (2) high-várzea = 0-1 mo/yr, maximum  
147 high-water levels < 1.5 m (n = 6); (3) mid-várzea = 2-4 mo/yr, maximum high-water levels = 1-2  
148 m (n = 6); and (4) low-várzea = 5-12 mo/yr, maximum high-water levels  $\geq$  2 m (n = 4). Flood  
149 depth within each plot was determined by measuring the height of visible watermarks left on tree

150 trunks within each plot after the most recent inundation peak. These measurements were made  
151 with a measuring tape to the nearest mm.

152 2.3. *Above-ground woody plant diversity:* We used 0.1 ha floristic plots (100 m x 10 m)  
153 placed perpendicular to the main river channel to minimize variability in flood depth and  
154 duration within plots. We inventoried woody plant diversity as described in Bredin et al. (2020).  
155 Briefly, within each floristic plot, all trees, hemiepiphytes, and palms  $\geq 10$ cm diameter at breast  
156 height (dbh) – as well as all high-climbing woody lianas  $\geq 5$  cm dbh – were measured and  
157 identified. Individuals that could not be determined to species level were sorted to morpho-  
158 species or, where applicable, higher taxonomic levels. For the following analyses we only  
159 retained floristic data from plots where we also obtained information about substrate biota (n =  
160 18).

161 2.4. *Below-ground microbial diversity:* To allow for comparisons with other studies of below-  
162 ground biodiversity, we used the sampling strategy described in Tedersoo et al. (2014) and Ritter  
163 et al. (2019b). Briefly, we superimposed 22 circular plots with a 28 m radius over the floristic  
164 plots by matching exactly the midpoints of the circular substrate plot with those of the  
165 rectangular floristic plots. Within each circular plot, we randomly selected 20 trees and collected  
166 litter and soil samples at the opposite sides of each stem. We first took a litter sample at every  
167 sampling point. After removing the leaf litter, we used a soil auger (2.5 cm in diameter) to collect  
168 the top 5 cm of the soil. In total, we collected litter and soil at 40 points per plot. The samples  
169 were then mixed to provide one composite litter sample and one composite soil sample per plot.  
170 For each plot, soil samples were divided into two parts. The first part was sun-dried and  
171 transported to the EMBRAPA laboratory in Manaus (Brazil) where physicochemical analyses  
172 were performed following standardized procedures (Donagema et al., 2011; Ritter et al., 2018).



173 The second part of the soil samples, as well as the litter samples, were dried with sterilized white  
174 silica gel 1–4 mm and transported to the University of Gothenburg, Sweden, for DNA extraction.

175 *2.5. DNA extraction and sequencing:* For total DNA extraction, we used the PowerMax® Soil  
176 DNA Isolation Kit (MO BIO Laboratories, USA) according to the manufacturer's instructions.  
177 We used 10 g (dry weight) from all soil samples and 15 ml of the litter samples (corresponding  
178 to 3–10 g of dry weight litter, depending on texture and composition). We checked DNA  
179 extraction quality and concentration in a Qubit 30® fluorimeter (Invitrogen, Sweden). The soil  
180 and litter samples from which DNA was successfully extracted were sent to Aimethods  
181 (Germany) for amplification and sequencing. We targeted prokaryotes with the V3-V4 region  
182 (~460 bases) of the 16S rDNA gene using the forward primer (5'-CCTACGGGN  
183 GGCWGCAG-3') and the reverse primer (5'-GACTACH VGGGTATCTAATCC-3') from  
184 Klindworth et al. (2013). Eukaryotes were targeted with the V7 region of the 18S rDNA gene  
185 using the forward and reverse primers (5'-TTTGTCTGSTTAATTSCG-3') and (5'-  
186 TCACAGACCTGTTATTGC-3') designed by Guardiola et al. (2015) to yield 100–110 bases  
187 long fragments. The 16S rDNA fragment was sequenced with the Illumina MiSeq 2×300  
188 platform, and the 18S rDNA fragment with Illumina Microarray 2×150. We sequenced negative  
189 controls in all steps: three for the extraction, two for the amplification, and two for the index  
190 ligation.

191 *2.6. Sequence analyses and taxonomic assessment:* We used the Cutadapt package (Martin,  
192 2011) in Python v.3.3 (Van Rossum and Drake, 2009) to remove primers. We then used the  
193 DADA2 package (Callahan et al., 2016) in R v. 4.0.2 (R Core Team, 2020) to quality filter reads,  
194 merge sequences, remove chimeras, and to infer amplicon sequence variants (ASVs). We  
195 excluded reads with ambiguous bases (maxN=0). Based on the quality scores of the forward and

196 reverse sequences, each read was required to have <3 or <5 errors, respectively (maxEE=c (3,5),  
197 truncQ=2). Therefore, ASVs were inferred for forward and reverse reads for each sample using  
198 the run-specific error rates. To assemble paired-end reads, we considered a minimum of 12 base  
199 pairs of overlap and excluded reads with mismatches in the overlapping region. Chimeras were  
200 removed using the consensus method of "removeBimeraDenovo" implemented in DADA2. We  
201 removed ASVs present in negative controls in a proportion larger than 40% of the reads for 18S  
202 and all ASVs present in negative control for 16S. We used the SILVAngs 132.1 reference  
203 database (Quast et al., 2012) for assessment of the taxonomic composition of the ASVs for both  
204 markers. The ASV reads by sample and taxonomic affiliation are provided in the Appendix 1  
205 (for 16S) and Appendix 2 (for 18S). Additionally, we identified the functional guild for the  
206 ASVs assigned to the fungal kingdom using the FungalTraits database (Polme et al., 2020).

207 *2.7. Statistical analysis:* We conducted all analyses in R using RStudio (2015). We used the  
208 tidyverse package v. 1.3.0 (Wickham, 2017) for data curation and ggplot2 v. 3.3.2 (Wickham,  
209 2016), ggfortify v. 0.4.11 (Tang et al., 2016), gridExtra v. 2.3 (Auguie and Antonov, 2016), and  
210 ggpubr v. 0.4.0 (Kassambara and Kassambara, 2020) for data visualisation (scripts in Appendix  
211 3).

212 *2.7.1. Soil properties* – To compare our results with other areas, we included the soil property  
213 data from terra firme and várzea in Benjamin Constant (far western Brazilian Amazonia) and  
214 Caxiuanã (far eastern Amazonia), available in Ritter et al. (2018), in our data analyses (Appendix  
215 4 Table A1). We first normalized all soil variables to zero mean and unit variance using the  
216 “scale” function of vegan v. 2.4-3 (Oksanen et al., 2010). We then performed a principal  
217 component analysis (PCA) to reduce the number of soil property variables for subsequent  
218 analyses and visualise soil physicochemical properties in relation to forest type and flood level

219 (i.e. terra firme, high-várzea, mid-várzea, low-várzea, or várzea where information on placement  
220 along the flooding gradient was absent).

221 2.7.2. Alpha diversity – As the richness estimates could be biased by rare ASVs (Haegeman et  
222 al., 2013), we calculated ASV Fisher’s alpha diversity (i.e., the relationship between the number  
223 of ASVs in any given plot and the number of reads of each ASV) using the phyloseq R package  
224 v.1.34.0 (McMurdie and Holmes, 2013) separately for the prokaryote (16S) and eukaryote (18S)  
225 datasets. For the woody plant communities, we used an abundance species matrix. We calculated  
226 the metrics within each plot and compared visually the non-normalized Fisher’s alpha diversity  
227 indices of the below-ground biota and above-ground plant communities. We analysed soil and  
228 litter Fisher’s alpha diversity as a function of flood level (modelled as a continuous variable  
229 represented by the measured floodwater marks on trees, with terra firme being zero, and  
230 categorically according to forest type, i.e. flood level), soil properties (represented by PC1 of the  
231 soil PCA), type of sample (litter or soil), and above-ground Fisher’s alpha diversity for woody  
232 plants. We normalized all the Fisher’s alpha diversities to zero mean and unit variance using the  
233 “scale” function in vegan. Thus, we defined a set of models to explain below-ground alpha  
234 diversity. The final model set included models with flood level, inundation depth of the last  
235 flood, PC1 from the soil properties PCA, type of sample (litter or soil) and woody plant Fisher’s  
236 alpha diversity as predictor variables, and additional models with interaction terms among the  
237 flood levels and sample types with woody plant Fisher’s alpha diversity and the flood levels with  
238 soil PC1. The final model set also included a constant, intercept-only model, comprising a total  
239 of nine models for each dependent variable (Table 1).

240 Models were selected using an information theory approach based on AIC (Akaike, 1974) and  
241 corrected AICs (AICc) for small sample sizes (Burnham and Anderson, 2002). Models with

242  $dAIC \leq 2$  were considered equally plausible, and we used the normalized model weight ( $w_i$ ) to  
243 contrast the best model to the constant (no-effect) model. We used generalized linear models  
244 (Crawley, 2007) with Gaussian error distributions after checking for the distributions of  
245 residuals. The GLM analyses were performed using the *vegan* package, and model selection was  
246 carried out using the *bbmle* package v.1.0.20 (Bolker and Bolker, 2017).

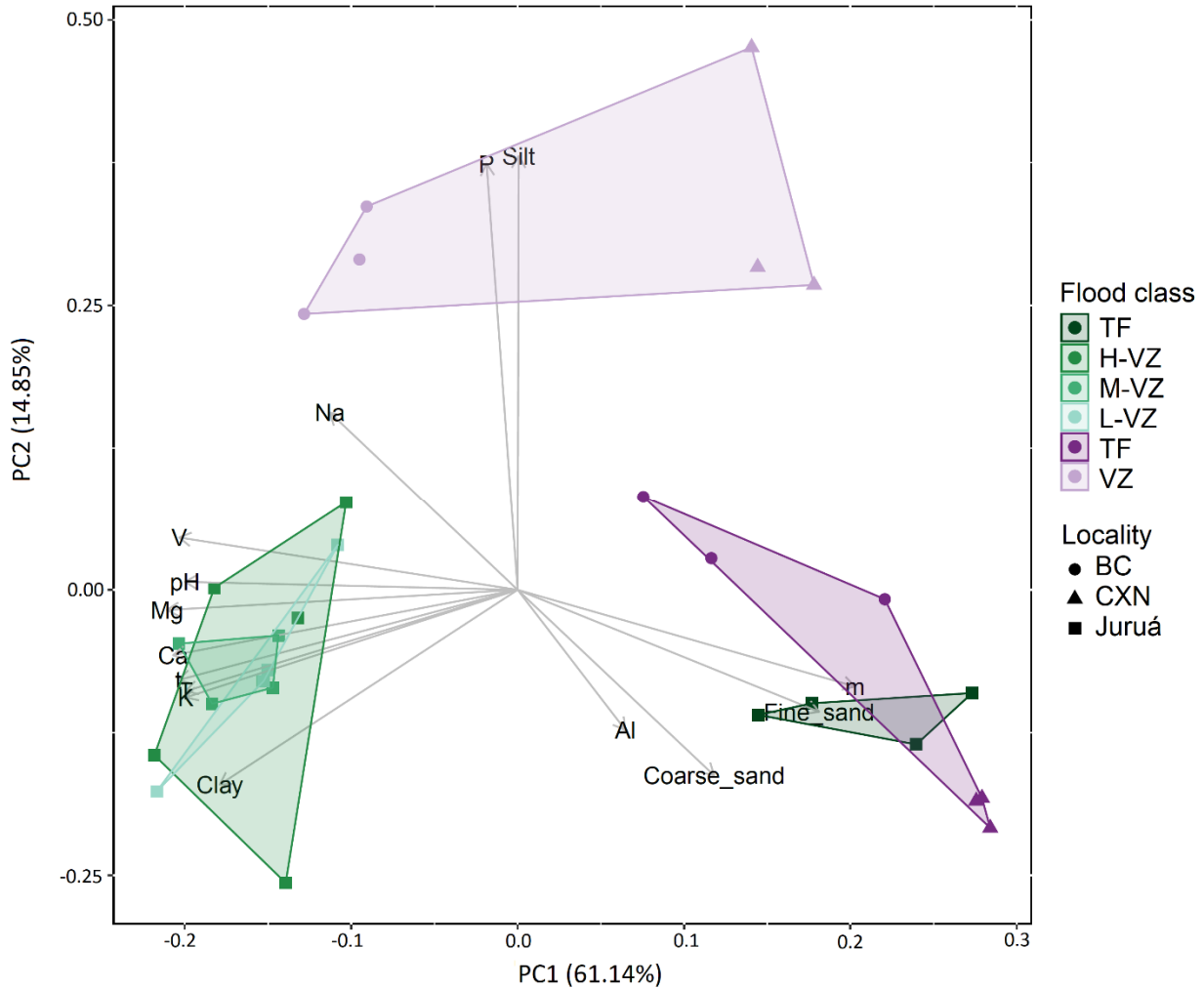
247 2.7.3. Beta diversity – We constructed two-dimensional non-metric multidimensional scaling  
248 (NMDS) ordinations of the abundance (reads) matrices of prokaryotes (16S) and eukaryotes  
249 (18S). We first transformed read counts using the ‘varianceStabilizingTransformation’ function  
250 in DESeq2 v.1.30.1 (Love et al., 2014) as suggested by McMurdie & Holmes (2013). This  
251 transformation normalizes the count data with respect to sample size (number of reads in each  
252 sample) and variances, based on fitted dispersion-mean relationships (Love et al., 2014). We  
253 then used the ‘metaMDS’ function and Bray-Curtis distances in the *vegan* package to assess  
254 community dissimilarity among all samples in the NMDS. We used the ‘envfit’ method in *vegan*  
255 to fit flood levels and sample types onto the NMDS ordination as a measure of the correlation  
256 among these factors with the NMDS axes. Additionally, we constructed two-dimensional non-  
257 metric multidimensional scaling (NMDS) ordinations based on the abundance data of the woody  
258 plants.

### 259 **3. Results**

260 We were able to extract, amplify, and sequence DNA for both prokaryotes (16S) and eukaryotes  
261 (18S) in 13 soil samples, 17 litter samples for prokaryotes (16S), and 16 litter samples for  
262 eukaryotes (18S). We obtained a total of 787,834 reads and 10,213 ASVs for the prokaryotes  
263 (16S). After removing the negative controls, we kept 757,827 reads and 9,337 ASVs. For the  
264 eukaryotes (18S), we obtained 616,237 reads belonging to 2,267 ASVs and we kept 572,953

265 reads belonging to 2,004 ASVs after removing the negative controls. See Appendix 4, Table A2  
266 for the number of reads and ASV richness for each plot, and Appendix 5 and 6 for krona charts  
267 of 16S and 18S taxonomic composition, respectively. The raw sequences are deposited in  
268 Genbank under the Bioproject PRJNA723037, BioSample SAMN18800640: Jurua (TaxID:  
269 410658), accession SRA numbers: SRR14286278 - SRR14286277.

270 *3.1. Soil properties:* The principal component analysis showed that edaphic properties varied  
271 between terra firme and várzea plots and that flood depth or duration had no apparent effect on  
272 várzea soil physicochemical composition (Fig. 2; Appendix 4 Table A3). Hence, várzea soils  
273 from Juruá largely overlapped (Fig. 2). Várzea soils were dominated by clay and silt, whereas  
274 terra firme soils were sandier (Fig 2). Terra firme soils were less fertile than várzea soils, with  
275 lower concentrations of important nutrients, such as potassium (K), calcium (Ca), and  
276 magnesium (Mg) (Fig 2). Compared with the terra firme and várzea soils from Benjamin  
277 Constant (far western Brazilian Amazonia) and Caxiuanã (far eastern Brazilian Amazonia), the  
278 Juruá várzea is characterized by more exchangeable bases and clay, and less phosphorous (P).  
279 The Juruá terra firme soils are placed between the Benjamin Constant and Caxiuanã terra firme  
280 soils (Fig. 2).

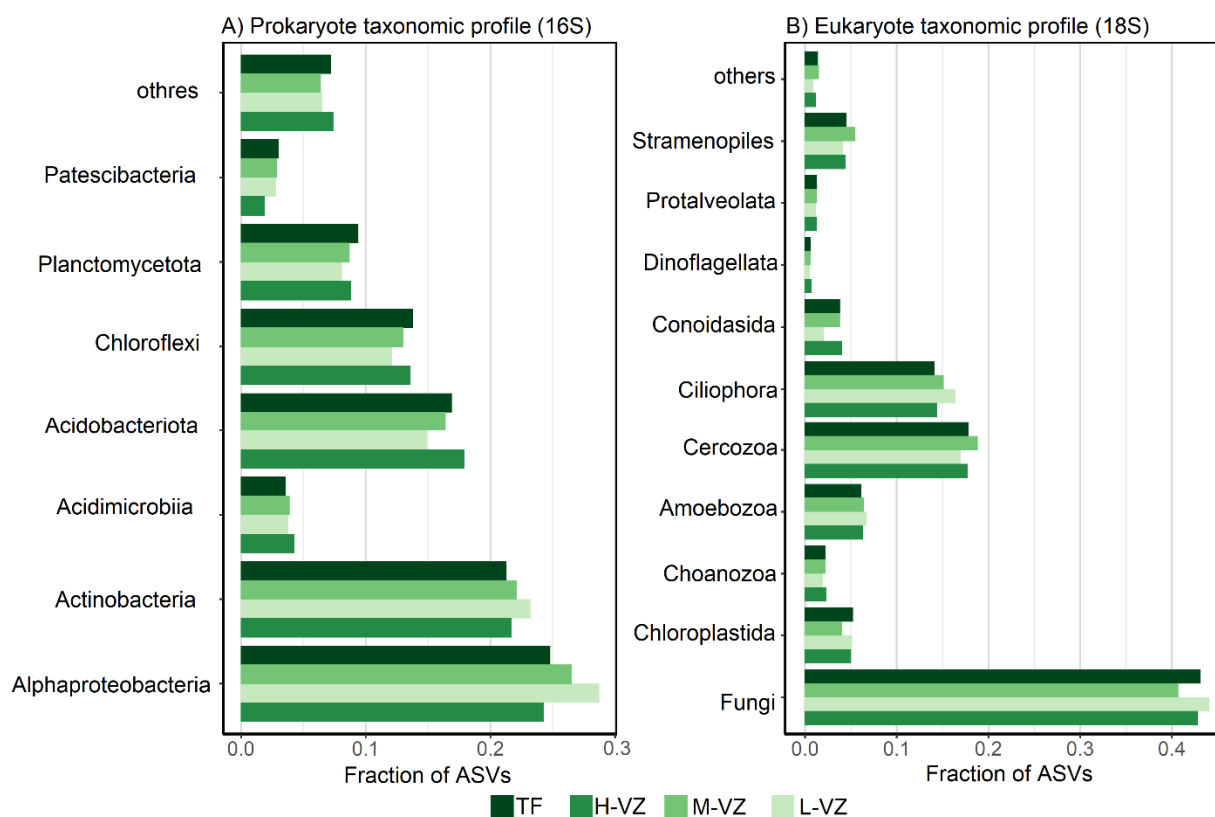


281

282 **Fig. 2.** Principal component analysis (PCA) showing the clustering of inventory plots along the  
283 first two PCA axes in relation to the soil physicochemical composition. The colours of the  
284 clusters reveal the geographic location (Juruá - this study - in green nuances; Benjamin Constant  
285 and Caxiuanã = purple) and the flooding gradient represented by the Juruá flood levels: TF:  
286 Terra firme; HV: High-várzea; MV: Mid-várzea; and LV: Low-várzea. The shape of the points  
287 indicates plot locality: Juruá = squares, Benjamin Constant = circle; and Caxiuanã = triangles.

288

289 3.2. *Below-ground taxonomic composition:* The taxonomic composition of the prokaryote  
 290 component shows that the groups with the highest number of ASVs were Alphaproteobacteria  
 291 (~25% of the taxa identified in our samples, equivalent to ~2000 ASVs per flood level; Fig. 3A;  
 292 Appendix 4 Fig. A1A), Actinobacteria (~23%, average ~1700 ASVs; Fig. 3A; Appendix 4 Fig.  
 293 A1A), and Acidobacteria (~18%, average ~1300 ASVs; Fig. 3A; Appendix 4 Fig. A1A). Among  
 294 eukaryotes, Fungi had the highest number of ASVs (~43%, ~600 ASVs), mainly Ascomycota  
 295 and Basidiomycota (Fig. 3B; Appendix 4 Fig. A1B) followed by Cercozoa (~18%, ~300 ASVs;  
 296 Fig. 3B; Appendix 4 Fig S1B) and Ciliophora (~15%, ~250 ASVs; Fig. 3B; Appendix 4 Fig  
 297 A1B). Most fungi were classified as saprotrophs (Appendix 4 Fig. A2). Other groups present  
 298 were pathogens, parasites, mycorrhizae fungi and unclassified (Appendix 4 Fig. A2).

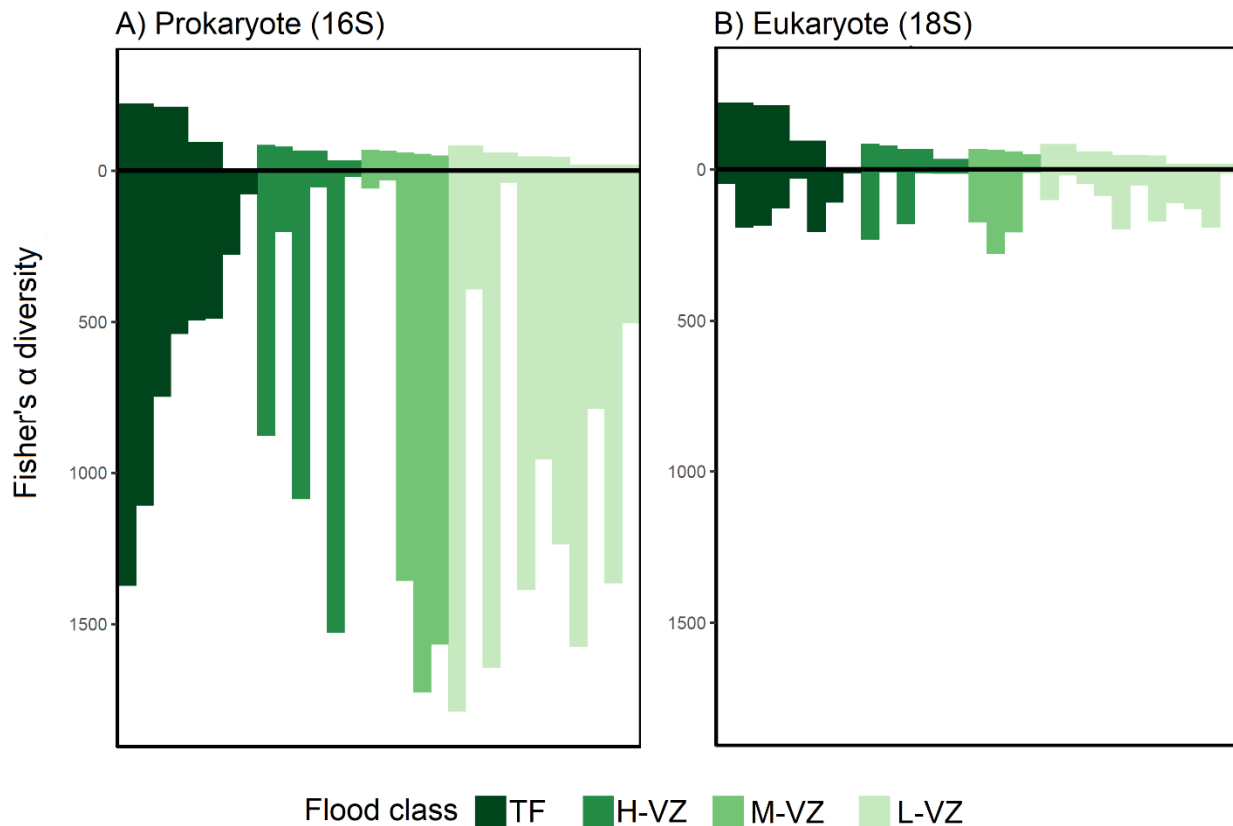


299

300 **Fig. 3:** Fraction of ASVs by taxonomic group and flood level for (A) prokaryotes and (B)  
301 eukaryotes. Flood levels are TF: Terra firme; H-VZ: High-várzea; M-VZ: Mid-várzea; and L-  
302 VZ: Low-várzea.

303  
304 *3.3. Alpha diversity:* We found that the best model to explain bacterial (16S) diversity  
305 included woody plant Fisher's alpha diversity and sample type (soil or litter) with an interaction  
306 effect between the two (Table 1), but only sample type was significant (Table 2). For eukaryotes  
307 (18S), three models had a delta AICc lower than 2 (Table 1). The first model ( $dAICc = 0$ )  
308 included only sample type, the second ( $dAICc = 1.1$ ) included only the woody plant Fisher's  
309 alpha diversity, and the third model ( $dAICc = 1.3$ ) included the woody plant Fisher's alpha  
310 diversity and sample type with an interaction effect between the two (Table 1). In all models,  
311 only sample type was significant (Table 2). Bacterial Fisher's alpha diversity was higher than the  
312 Fisher's alpha diversity of either eukaryotes or woody plants. In terra firme, bacterial diversity in  
313 soil and litter, but not eukaryotes, appears to correlate with woody plant diversity. For várzea, no  
314 pattern was observed (Fig. 4).





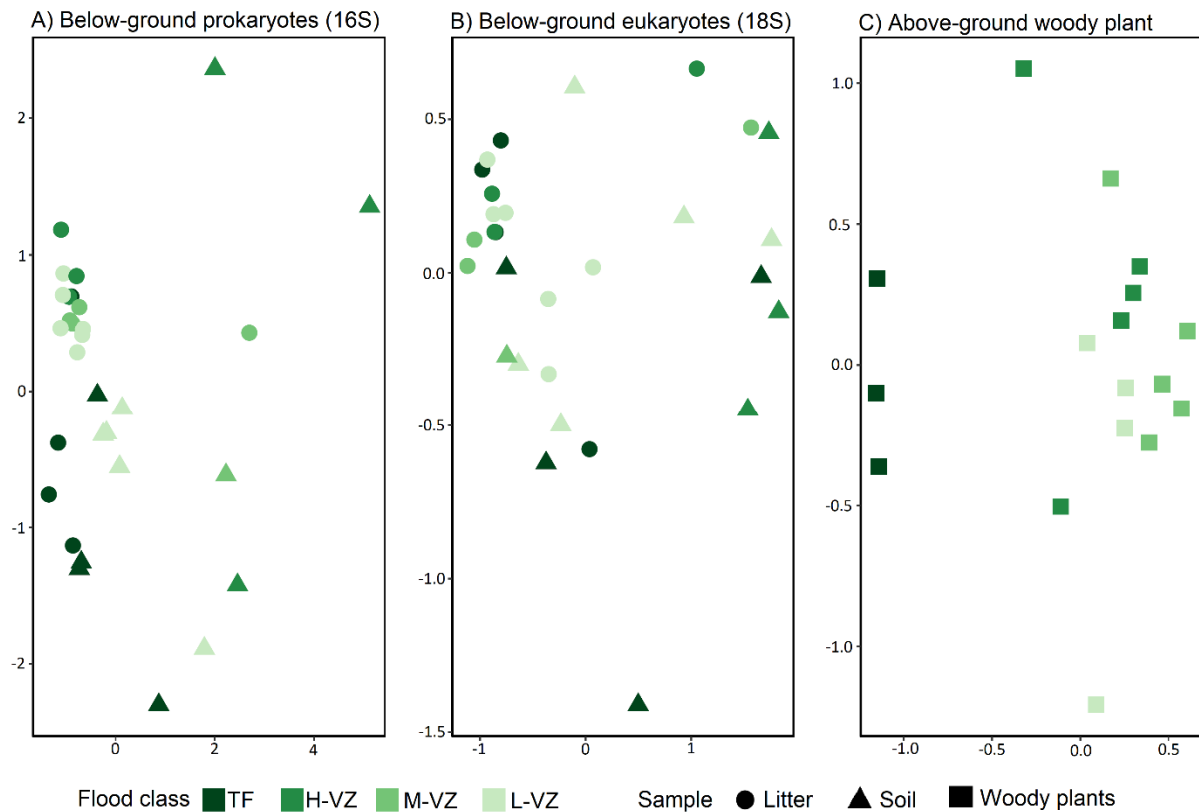
315

316 **Fig. 4.** Above-ground woody plant Fisher's alpha diversity *versus* below-ground Fisher's alpha  
317 diversity of A) prokaryotic (16S) and B) eukaryotic (18S) organisms in Juruá litter and soil  
318 samples. Prokaryotic and eukaryotic diversity are shown in negative values. Woody plant  
319 diversity is shown in positive values. Flood levels are TF: Terra firme; H-VZ: High-várzea; M-  
320 VZ: Mid-várzea; and L-VZ: Low-várzea.

321

322 *3.4. Beta diversity:* Community compositions were similar among plots across flood levels  
323 and sample types (litter and soil). For bacteria, there is a grouping of terra firme plots with some  
324 overlap with várzea plots (Fig. 5A). No clear pattern was observed for soil eukaryotes (Fig. 5B).  
325 For woody plant communities, there is a turnover in species compositions across different flood

326 levels (Fig. 5C). The envfit test indicated a significant effect of flood level on both the  
327 prokaryote ( $R^2 = 0.24$ ;  $p = 0.022$ ) and woody plant ( $R^2 = 0.48$ ;  $p = 0.003$ ) communities, but not  
328 for soil eukaryotes ( $R^2 = 0.14$ ;  $p = 0.28$ ). The envfit test also indicated a significant effect of  
329 sample type on the prokaryote ( $R^2 = 0.25$ ;  $p = 0.001$ ) and eukaryote ( $R^2 = 0.22$ ;  $p = 0.006$ )  
330 communities.



332 **Fig. 5. Community structure in relation to substrate type and flood levels.** Visualisation of  
333 non-metric multidimensional scaling (NMDS) for (A) prokaryotes (16S), (B) eukaryotes (18S),  
334 and (C) woody plants using Bray-Curtis dissimilarity indices. Symbols represent different  
335 substrates (i.e. sample types) where filled circles = litter samples and filled triangles = soil  
336 samples. Colours represent the different flood levels: TF = Terra firme; H-VZ = High-várzea; M-  
337 VZ = Mid-várzea; and L-VZ = Low-várzea.

338

#### 339 **4. Discussion**

340 Our analyses have documented, for the first time, the degree to which soil and litter biota  
341 biodiversity are affected by the flooding gradient in central-western Amazonian forests of  
342 varying floristic diversity. We show a weak correlation between soil and litter community  
343 composition and inundation period but find that below-ground Fisher's alpha diversity cannot be  
344 explained by the flooding gradient. We also show that the edaphic properties differed between  
345 terra firme and várzea, but not among várzea forests along the flooding gradient.

346 *4.1. Edaphic properties:* Várzea edaphic properties in the Juruá differed from the other two  
347 Amazonian várzeas that we included in our analyses (Fig. 2). For instance, the Juruá várzea was  
348 poorer in phosphorus (P) and silt, but rich in magnesium (Mg), calcium (Ca), potassium (K), and  
349 clay. This high-density clay content in the Juruá várzea may act as a physical barrier to water  
350 infiltration. On the other hand, clayey soils also have a high water holding capacity (Hillel,  
351 2013), which prevents it from drying out completely during the non-flooded periods. The high  
352 clay content additionally made várzea samples hard to collect and to break once dried. Possibly,  
353 this was the main factor that hindered DNA extraction in our study.

354 Compared to the terra firme soils, the Juruá várzea soils were more fertile, presumably due to the  
355 yearly inflow of nutrient-rich alluvial sediments by the Juruá River. Moreover, the Juruá terra  
356 firme soils presented similar edaphic properties to those of the terra firme forests in Benjamin  
357 Constant and Caxiuanã. This was unexpected since the terra firme forest that we sampled in the  
358 Juruá grow on paleo-várzea sediments (Assis et al., 2015), and therefore presumably should have  
359 been relatively nutrient rich compared to typically well-drained and heavily leached terra firme

360 soils on older geological formations (Sombroek, 2000). However, these soils presented similar  
361 edaphic properties to those of the terra firme forests in Benjamin Constant and Caxiuanã,  
362 suggesting that nutrients are soon leached from várzea substrates once they no longer experience  
363 flooding and an influx of river sediments.

364 *4.2. Below-ground taxonomic composition:* Alphaproteobacteria and Planctomycetes were  
365 abundant in our samples, accounting for 40% of our 16S data (Fig. 3A). These groups are known  
366 to be very diverse in undisturbed forests (de Carvalho et al., 2016) and they are generally  
367 common in Amazonian soils (Ritter et al., 2019b; Zinger et al., 2019). Interestingly, other  
368 bacterial groups commonly found in Amazonian soils (Ritter et al., 2019b; Zinger et al., 2019)  
369 and elsewhere (Delgado-Baquerizo et al., 2018) – notably Betaproteobacteria and Bacteroidetes -  
370 were not present in the Juruá samples. Because these groups are known from a diverse range of  
371 habitats, including várzea and terra firme, this surprised us and clearly highlight that we have  
372 much to discover about Amazonian soil biodiversity.

373 Patescibacteria (e.g., the candidate phyla radiation group), not previously reported in other  
374 várzea soils, were found in the Juruá samples (Fig. 3A). This group was recently described  
375 (Brown et al., 2015) and until now it had only been registered in Amazonian pasture soils  
376 (Lemos et al., 2020). An interesting characteristic of Patescibacteria is the small size of their  
377 genomes (usually <1.5 Mbp) and their lack of biosynthetic capabilities (Brown et al., 2015).  
378 These characteristics indicate that they could be co-metabolic interdependent (He et al., 2015;  
379 Lemos et al., 2019). Such interdependencies with other organisms would suggest a restrict  
380 occurrence or different functionality dependent on the community in which they occur. Yet,  
381 Patescibacteria show similar functional profiles under distinct climate conditions (tropical soils  
382 and permafrost; Lemos et al., 2020). Although their apparent plasticity is interesting, very little

383 information is available for this group. The design of new 16S rRNA gene primers that better  
384 amplify Patescibacteria is required to elucidate the ecology and distribution of Patescibacteria in  
385 Amazonian soils and worldwide. Additionally, analysis of metatranscriptomes could improve our  
386 understanding of the metabolism in Patescibacteria and other bacteria under different substrate  
387 conditions.

388 Among the eukaryotes, we found a higher proportion of fungi in the Juruá substrates than  
389 previously documented for other areas in Amazonia (Ritter et al., 2019b). Whereas Ritter et al.  
390 (2020) found fewer fungi in várzea than in other environments, we found more fungi in várzea  
391 than in the adjacent terra firme, most of which were saprotrophs (Appendix 4 Fig. A2). Singer et  
392 al. (1983) hypothesized that ectomycorrhizal fungi increase the ability of their host plants to  
393 acquire nutrients and water in low-fertility soils, such as in the Amazonian sandy-soil  
394 ecosystems. However, we found very few ectomycorrhizal fungi in both várzea (more fertile)  
395 and terra firme (less fertile; Appendix 4 Fig. A2). Yet, around 35% of the fungi could be not  
396 assigned to any functional guild. This makes comparisons difficult and highlights the need to  
397 further investigate Amazonian soil biodiversity and its ecology.

398 Some eukaryotic groups detected in other Amazonian localities by the same 18S primers as the  
399 ones used here (Ritter et al., 2019b; Zinger et al., 2019), were absent in the Juruá samples. Such  
400 groups include nematodes and arthropods (Fig. 2B). Although the 18S primers that we used are  
401 not optimal for sequencing animals, it was surprising not to find these groups in our samples  
402 (except for one nematode sequence in várzea and terra firme). Low nematode diversity in  
403 Amazonian várzeas was previously reported by Cares (1984). One reason for the absence of  
404 these animals in várzea substrates could be that the high amount of clay in the soil and the  
405 seasonal floods, make várzea soil and litter unfit for nematode occupation. However, this does

406 not explain the absence of soil animals in our terra firme samples since these were relatively  
407 clay-free and unflooded. To test this hypothesis, we need further studies in soils with a gradual  
408 difference in clay proportion and specific primers targeting nematodes (e.g. Kawanobe et al.,  
409 2021) alongside morphological examination of the diversity in the samples.

410 *4.3. Above- versus below-ground diversity:* There was no relationship between above- and  
411 below-ground alpha diversity across the different forest types included in this study. This  
412 mismatch could be explained by the flood pulse that may have masked any pattern by carrying  
413 organisms across all flood levels. A lack of clear relationships between above- and below-ground  
414 biodiversity has previously been demonstrated globally (Cameron et al., 2019) and for other  
415 Amazonian areas (Ritter et al., 2019a). However, for Amazonia this mismatch was partial.  
416 Across habitats, no correspondence was found between below-ground prokaryote or eukaryote  
417 alpha diversity and above-ground bird or tree alpha diversity (Ritter et al., 2019a). Nevertheless,  
418 there was a gradual decrease in below- and above-ground alpha diversity from the west to the  
419 east across the Amazon basin (Ritter et al., 2019a). Indeed, bacterial diversity appears to  
420 correlate with woody plant diversity in terra firme forests (Fig. 3A), but due to the sample  
421 limitation, just four terra firme plots, we could not find a significance in this relationship.

422 *4.4 Flooding gradient and community composition:* Most ASVs occur throughout the  
423 flooding gradient (Appendix 1 and 2). This result was partly expected since the seasonal flood  
424 waters could carry DNA (e.g. of inactive spores, dead or living organisms) across all várzea  
425 flood levels. Yet, the bacterial community composition of the Juruá substrate varied with flood  
426 level and woody plant diversity. This result indicates that below-ground bacteria may present  
427 different tolerances to hydrological stressors and or interdependencies with certain woody plant  
428 species. For instance, nodulation caused by nitrogen fixing bacteria are more frequent in

429 Amazonian seasonally flooded forests, indicating that nodulation may be favored in flooded  
430 areas (Parolin and Wittmann, 2010).

431

## 432 **5. Conclusion**

433 This is the first study to investigate the degree to which soil and litter biota are affected by the  
434 flooding gradient in Amazonian forests. In fact, as far as we are aware, substrates from only six  
435 other Amazonian várzeas have previously been investigated using a metabarcoding approach,  
436 and these studies did not consider the flooding gradient (Ritter et al., 2019b, 2019a; Ritter, 2018).  
437 Hence, the DNA barcoding data herein – consisting of a total of 19,550 ASVs, from 14 várzea  
438 and four terra firme plots – more than doubles the total database from Amazonian várzeas  
439 available to date. Considering the extent of lowland Amazonian floodplain forests, approx.  
440 516,000 km<sup>2</sup> (Hess et al., 2015), the need for more data from different geographical areas is  
441 obvious.

442 Studying below-ground communities along complex environmental gradients, like the one in the  
443 present study, offers an excellent opportunity to explore the responses of substrate biota to  
444 varying degrees of environmental stressors. Such studies can further our understanding of the  
445 patterns in below-ground biodiversity, their roles in the dynamics of seasonally flooded forests,  
446 and how these communities might respond to anthropogenic pressure and climate change.  
447 Therefore, the characterization of below-ground biodiversity in flooded forests, has theoretical  
448 implications for elucidating the patterns of biological diversity distribution. Practical  
449 implications include the identification of strategically important areas or areas of greater  
450 environmental sensitivity, for the conservation of biological diversity in face of environmental

451 change. This not trivial, as infrastructural development (e.g. hydroelectric dams) and climate  
452 change (more frequent extreme floods and droughts) are severely affecting the natural flood  
453 pulse and threaten the ecological integrity of seasonally flooded forests across Amazonia (Gloor  
454 et al., 2013; Junk et al., 2018; Latrubesse et al., 2020). Increased pressures in these ecosystems  
455 highlight the urgency for more studies of this kind to improve our understanding of biodiversity  
456 patterns and community structures as these will allow us to better foresee and mitigate climate  
457 change impacts on ecosystem functions.

458

459 **Acknowledgements:** This publication is part of the Projeto Médio Juruá series on Resource  
460 Management in Amazonian Reserves ([www.projetoediojuruu.org](http://www.projetoediojuruu.org)). We thank the Secretaria do  
461 Estado do Meio Ambiente e Desenvolvimento Sustentável do Amazonas (SEMA - DEMUC) and  
462 Instituto Brasileiro do Meio Ambiente e Recursos Naturais Renováveis (IBAMA)/Instituto Chico  
463 Mendes de Conservação da Biodiversidade (ICMBio) for authorising the research n°60/2016  
464 (RDS Uacari) and n°55077-1 (RESEX Médio Juruá). We are grateful to the members from the  
465 Projeto Médio Juruá team for logistical support. We thank Rita Homem Pelicano for dedicated  
466 soil sampling in the field! We thank Michael J.G. Hopkins, Rafael Leandro de Assis and Juliana  
467 Schietti with colleagues at INPA for providing logistical assistance and a place to work in  
468 Manaus. We thank Paulo Apóstolo Costa Lima Assunção (in memoriam) and Alexandro Elias  
469 dos Santos, assisted by Lorena M. Rincón, for identifying the woody plant species in the field  
470 and at the National Institute for Amazonia Research (INPA). We thank our local field assistants,  
471 Associação dos Produtores Rurais de Carauari (ASPROC), Operação Amazônia Nativa (OPAN),  
472 and the people of the central Juruá who in various ways assisted us throughout our work. Finally,



473 we thank Heléne Aronson and Katarzyna Wojnicka at the University of Gothenburg for  
474 quantifying the sampled DNA.

475 **Funding:** Y.K.B. was financed by the Norwegian University of Life Sciences (NMBU) as part  
476 of their PhD program in tropical ecology and an internal travel grant from NMBU. CDR was  
477 supported by the Alexander von Humboldt Foundation.

478

479 **References:**

- 480 Akaike, H., 1974. A new look at the statistical model identification, in: Selected Papers of  
481 Hirotugu Akaike. Springer, pp. 215–222.
- 482 Assis, R.L., Haugaasen, T., Schöngart, J., Montero, J.C., Piedade, M.T.F., Wittmann, F., 2015.  
483 Patterns of tree diversity and composition in Amazonian floodplain paleo- várzea forest.  
484 Journal of Vegetation Science 26, 312–322.
- 485 Auguie, B., Antonov, A., 2016. gridExtra: Miscellaneous functions for “grid” graphics (Version  
486 2.2. 1)[Computer software].
- 487 Bardgett, R.D., Van Der Putten, W.H., 2014. Belowground biodiversity and ecosystem  
488 functioning. Nature 515, 505–511.
- 489 Bolker, B., Bolker, M. Ben, 2017. Package ‘bbmle.’ Tools for General Maximum Likelihood  
490 Estimation 641.
- 491 Bredin, Y.K., Hawes, J.E., Peres, C.A., Haugaasen, T., 2020. Structure and Composition of Terra  
492 Firme and Seasonally Flooded Várzea Forests in the Western Brazilian Amazon. Forests 11,  
493 1361.
- 494 Brown, C.T., Hug, L.A., Thomas, B.C., Sharon, I., Castelle, C.J., Singh, A., Wilkins, M.J.,  
495 Wrighton, K.C., Williams, K.H., Banfield, J.F., 2015. Unusual biology across a group  
496 comprising more than 15% of domain Bacteria. Nature 523, 208–211.
- 497 Burnham, K.P., Anderson, D.R., 2002. Model selection and.
- 498 Callahan, B.J., McMurdie, P.J., Rosen, M.J., Han, A.W., Johnson, A.J.A., Holmes, S.P., 2016.

- 499 DADA2: high-resolution sample inference from Illumina amplicon data. *Nature Methods*  
500 13, 581–583.
- 501 Cameron, E.K., Martins, I.S., Lavelle, P., Mathieu, J., Tedersoo, L., Bahram, M., Gottschall, F.,  
502 Guerra, C.A., Hines, J., Patoine, G., Siebert, J., Winter, M., Cesarz, S., Ferlian, O., Kreft,  
503 H., Lovejoy, T.E., Montanarella, L., Orgiazzi, A., Pereira, H.M., Phillips, H.R.P., Settele, J.,  
504 Wall, D.H., Eisenhauer, N., 2019. Global mismatches in aboveground and belowground  
505 biodiversity. *Conservation Biology* 0, 1–6. doi:10.1111/cobi.13311
- 506 Cares, J.E., 1984. Fauna fitonematologica de varzea e terra firme nas proximidades de Manaus-  
507 AM. UNB.
- 508 Castello, L., Macedo, M.N., 2016. Large-scale degradation of Amazonian freshwater  
509 ecosystems. *Global Change Biology* 22, 990–1007.
- 510 Crawley, M.J., 2007. Generalized linear models. *The R Book* 511–526.
- 511 Creer, S., Deiner, K., Frey, S., Porazinska, D., Taberlet, P., Thomas, W.K., Potter, C., Bik, H.M.,  
512 2016. The ecologist’s field guide to sequence-based identification of biodiversity. *Methods*  
513 in *Ecology and Evolution* 7, 1008–1018. doi:10.1111/2041-210X.12574
- 514 de Carvalho, T.S., Jesus, E. da C., Barlow, J., Gardner, T.A., Soares, I.C., Tiedje, J.M., Moreira,  
515 F.M. de S., 2016. Land use intensification in the humid tropics increased both alpha and  
516 beta diversity of soil bacteria. *Ecology* 97, 2760–2771.
- 517 Delgado-Baquerizo, M., Oliverio, A.M., Brewer, T.E., Benavent-González, A., Eldridge, D.J.,  
518 Bardgett, R.D., Maestre, F.T., Singh, B.K., Fierer, N., 2018. A global atlas of the dominant

- 519 bacteria found in soil. *Science* 359, 320–325. doi:10.1126/science.aap9516
- 520 Delgado-Baquerizo, M., Reich, P.B., Trivedi, C., Eldridge, D.J., Abades, S., Alfaro, F.D.,  
521 Bastida, F., Berhe, A.A., Cutler, N.A., Gallardo, A., 2020. Multiple elements of soil  
522 biodiversity drive ecosystem functions across biomes. *Nature Ecology & Evolution* 4, 210–  
523 220.
- 524 Donagema, G.K., De Campos, D.B., Calderano, S.B., Teixeira, W.G., Viana, J.M., 2011. Manual  
525 de métodos de análise de solo, Embrapa Solos-Documentos (INFOTECA-E). Rio de  
526 Janeiro.
- 527 García-Palacios, P., Maestre, F.T., Kattge, J., Wall, D.H., 2013. Climate and litter quality  
528 differently modulate the effects of soil fauna on litter decomposition across biomes.  
529 *Ecology Letters* 16, 1045–1053.
- 530 Gloor, M., Brienen, R.J.W., Galbraith, D., Feldpausch, T.R., Schöngart, J., Guyot, J., Espinoza,  
531 J.C., Lloyd, J., Phillips, O.L., 2013. Intensification of the Amazon hydrological cycle over  
532 the last two decades. *Geophysical Research Letters* 40, 1729–1733.
- 533 Guardiola, M., Uriz, M.J., Taberlet, P., Coissac, E., Wangenstein, O.S., Turon, X., 2015. Deep-  
534 sea, deep-sequencing: metabarcoding extracellular DNA from sediments of marine canyons.  
535 *PLoS One* 10, e0139633.
- 536 Haegeman, B., Hamelin, J., Moriarty, J., Neal, P., Dushoff, J., Weitz, J.S., 2013. Robust  
537 estimation of microbial diversity in theory and in practice. *The ISME Journal* 7, 1092.
- 538 Hättenschwiler, S., Gasser, P., 2005. Soil animals alter plant litter diversity effects on

- 539 decomposition. *Proceedings of the National Academy of Sciences* 102, 1519–1524.
- 540 Haugaasen, T., Peres, C.A., 2006. Floristic, edaphic and structural characteristics of flooded and  
541 unflooded forests in the lower Rio Purús region of central Amazonia, Brazil. *Acta*  
542 *Amazonica* 36, 25–35.
- 543 Hawes, J.E., Peres, C.A., 2016. Patterns of plant phenology in Amazonian seasonally flooded  
544 and unflooded forests. *Biotropica* 48, 465–475. doi:10.1111/btp.12315
- 545 He, X., McLean, J.S., Edlund, A., Yooseph, S., Hall, A.P., Liu, S.-Y., Dorrestein, P.C.,  
546 Esquenazi, E., Hunter, R.C., Cheng, G., 2015. Cultivation of a human-associated TM7  
547 phylotype reveals a reduced genome and epibiotic parasitic lifestyle. *Proceedings of the*  
548 *National Academy of Sciences* 112, 244–249.
- 549 Hess, L.L., Melack, J.M., Affonso, A.G., Barbosa, C., Gastil-Buhl, M., Novo, E.M.L.M., 2015.  
550 Wetlands of the lowland Amazon basin: Extent, vegetative cover, and dual-season  
551 inundated area as mapped with JERS-1 synthetic aperture radar. *Wetlands* 35, 745–756.
- 552 Johnson, N.C., Gehring, C., Jansa, J., 2016. Mycorrhizal mediation of soil: fertility, structure,  
553 and carbon storage. Elsevier.
- 554 Julião, G.R., Venticinque, E.M., Fernandes, G.W., 2018. Influence of Flood Levels on the  
555 Richness and Abundance of Galling Insects Associated with Trees from Seasonally Flooded  
556 Forests of Central Amazonia, Brazil, in: *Igapó (Black-Water Flooded Forests) of the*  
557 *Amazon Basin*. Springer, pp. 99–117.
- 558 Junk, W., 1989. Flood tolerance and tree distribution in central Amazonian floodplains. *Holm-*

- 559 nielsen. *Tropical Forests; Botanical Dynamics, Speciation, and Diversity*: 47–64.
- 560 Junk, W.J., Piedade, M.T.F., da Cunha, C.N., Wittmann, F., Schöngart, J., 2018. Macrohabitat  
561 studies in large Brazilian floodplains to support sustainable development in the face of  
562 climate change. *Ecohydrology & Hydrobiology* 18, 334–344.
- 563 Kassambara, A., Kassambara, M.A., 2020. Package ‘ggpubr.’
- 564 Kawanobe, M., Toyota, K., Ritz, K., 2021. Development and application of a DNA  
565 metabarcoding method for comprehensive analysis of soil nematode communities. *Applied*  
566 *Soil Ecology* 166, 103974.
- 567 Klindworth, A., Pruesse, E., Schweer, T., Peplies, J., Quast, C., Horn, M., Glöckner, F.O., 2013.  
568 Evaluation of general 16S ribosomal RNA gene PCR primers for classical and next-  
569 generation sequencing-based diversity studies. *Nucleic Acids Research* 41, e1–e1.
- 570 Kubitzki, K., 1990. Themes of diversification in neotropical forest. *Quimica Nova* 13, 4.
- 571 Latrubesse, E.M., d’Horta, F.M., Ribas, C.C., Wittmann, F., Zuanon, J., Park, E., Dunne, T.,  
572 Arima, E.Y., Baker, P.A., 2020. Vulnerability of the biota in riverine and seasonally flooded  
573 habitats to damming of Amazonian rivers. *Aquatic Conservation: Marine and Freshwater*  
574 *Ecosystems*.
- 575 Lemos, L.N., Manoharan, L., Mendes, L.W., Venturini, A.M., Pylro, V.S., Tsai, S.M., 2020.  
576 Metagenome assembled  $\square$  genomes reveal similar functional profiles of CPR/Patescibacteria  
577 phyla in soils. *Environmental Microbiology Reports* 12, 651–655.
- 578 Lemos, L.N., Medeiros, J.D., Dini  $\square$  Andreote, F., Fernandes, G.R., Varani, A.M., Oliveira, G.,

- 579 Pylro, V.S., 2019. Genomic signatures and co-occurrence patterns of the ultra-small  
580 Saccharimonadia (phylum CPR/Patescibacteria) suggest a symbiotic lifestyle. *Molecular*  
581 *Ecology* 28, 4259–4271.
- 582 Love, M.I., Huber, W., Anders, S., 2014. Moderated estimation of fold change and dispersion for  
583 RNA-seq data with DESeq2. *Genome Biology* 15, 550.
- 584 Maretti, C.C., 2014. Amazon: There is Hope! If we all do ‘the right thing’...; Deforestation,  
585 Protected Areas and Indigenous Territories: Past, evolution and... Which future? Brasilia.
- 586 Martin, M., 2011. Cutadapt removes adapter sequences from high-throughput sequencing reads.  
587 *EMBnet. Journal* 17, 10–12.
- 588 McMurdie, P.J., Holmes, S., 2013. phyloseq: an R package for reproducible interactive analysis  
589 and graphics of microbiome census data. *PloS One* 8, e61217.
- 590 Moura, M.R., Jetz, W., 2021. Shortfalls and opportunities in terrestrial vertebrate species  
591 discovery. *Nature Ecology & Evolution* 1–9.
- 592 Myster, R.W., 2016. The physical structure of forests in the Amazon Basin: a review. *The*  
593 *Botanical Review* 82, 407–427.
- 594 Oksanen, J., Blanchet, F.G., Kindt, R., Legendre, P., O’hara, R.B., Simpson, G.L., Solymos, P.,  
595 Stevens, M.H.H., Wagner, H., 2010. Vegan: community ecology package. R package  
596 version 1.17-4. [Http://Cran. r-Project. Org](http://Cran.r-Project.Org)>. Acesso Em 23, 2010.
- 597 Parolin, P. de, De Simone, O., Haase, K., Waldhoff, D., Rottenberger, S., Kuhn, U., Kesselmeier,  
598 J., Kleiss, B., Schmidt, W., Pledade, M.T.F., 2004. Central Amazonian floodplain forests:

- 599 tree adaptations in a pulsing system. *The Botanical Review* 70, 357–380.
- 600 Parolin, P., Wittmann, F., 2010. Struggle in the flood: tree responses to flooding stress in four  
601 tropical floodplain systems. *AoB Plants* 2010.
- 602 Pereira, P., Bogunovic, I., Muñoz-Rojas, M., Brevik, E.C., 2018. Soil ecosystem services,  
603 sustainability, valuation and management. *Current Opinion in Environmental Science &*  
604 *Health* 5, 7–13.
- 605 Petit, R.J., Hampe, A., 2006. Some evolutionary consequences of being a tree. *Annu. Rev. Ecol.*  
606 *Evol. Syst.* 37, 187–214.
- 607 Pietramellara, G., Ascher, J., Ceccherini, M.T., Renella, G., 2002. Soil as a biological system.  
608 *Annals of Microbiology* 52, 119–132.
- 609 Polme, S., Abarenkov, K., Nilsson, R.H., Lindahl, B.D., Clemmensen, K.E., Kauserud, H.,  
610 Nguyen, N., Kjøller, R., Bates, S.T., Baldrian, P., 2020. FungalTraits: a user-friendly traits  
611 database of fungi and fungus-like stramenopiles. *Fungal Diversity* 105, 1–16.
- 612 Prance, G.T., 1996. Islands in Amazonia. *Philosophical Transactions of the Royal Society of*  
613 *London. Series B: Biological Sciences* 351, 823–833.
- 614 Prance, G.T., 1979. Notes on the vegetation of Amazonia III. The terminology of Amazonian  
615 forest types subject to inundation. *Brittonia* 31, 26–38.
- 616 Quast, C., Pruesse, E., Yilmaz, P., Gerken, J., Schweer, T., Yarza, P., Peplies, J., Glöckner, F.O.,  
617 2012. The SILVA ribosomal RNA gene database project: improved data processing and  
618 web-based tools. *Nucleic Acids Research* 41, D590–D596.



- 619 R Core Team, 2020. R: the R project for statistical computing. 2019. URL: <https://www.R-Project.Org/>[Accessed 2020-03-30].
- 620
- 621 Ramalho, W.P., Andrade, M.S., Matos, L.R.A. de, Vieira, L.J.S., 2016. Amphibians of varzea  
622 environments and floating meadows of the oxbow lakes of the Middle Purus River,  
623 Amazonas, Brazil. *Biota Neotropica* 16.
- 624 Ríos-Villamizar, E.A., Adeney, J.M., Piedade, M.T.F., Junk, W.J., 2020. New insights on the  
625 classification of major Amazonian river water types. *Sustainable Water Resources  
626 Management* 6, 1–16.
- 627 Ritter, C.D., Dunthorn, M., Anslan, S., Xavier, V., Tedersoo, L., Henrik, R., Antonelli, A., 2020.  
628 Advancing biodiversity assessments with environmental DNA: Long-read technologies  
629 help reveal the drivers of Amazonian fungal diversity 00, 1–16. doi:10.1002/ece3.6477
- 630 Ritter, C.D. et al., 2018. High-throughput metabarcoding reveals the effect of physicochemical  
631 soil properties on soil and litter biodiversity and community turnover across Amazonia.  
632 *PeerJ* 6.
- 633 Ritter, C.D., Faurby, S., Bennett, D.J., Naka, L.N., ter Steege, H., Zizka, A., Haenel, Q., Nilsson,  
634 R.H., Antonelli, A., 2019a. The pitfalls of biodiversity proxies: Differences in richness  
635 patterns of birds, trees and understudied diversity across Amazonia. *Scientific Reports* 9.  
636 doi:10.1038/s41598-019-55490-3
- 637 Ritter, C.D., McCrate, G., Nilsson, R.H., Fearnside, P.M., Palme, U., Antonelli, A., 2017.  
638 Environmental impact assessment in Brazilian Amazonia: Challenges and prospects to  
639 assess biodiversity. *Biological Conservation* 206, 161–168.

640 doi:10.1016/j.biocon.2016.12.031

641 Ritter, C.D., Zizka, A., Barnes, C., Nilsson, R.H., Roger, F., Antonelli, A., 2019b. Locality or  
642 habitat? Exploring predictors of biodiversity in Amazonia. *Ecography* 42, 321–333.

643 doi:10.1111/ecog.03833

644 Ritter, C.D., Zizka, A., Roger, F., Tuomisto, H., Barnes, C., Nilsson, R.H., Antonelli, A., 2018.

645 High-throughput metabarcoding reveals the effect of physicochemical soil properties on soil  
646 and litter biodiversity and community turnover across Amazonia. *PeerJ* 2018, e5661.

647 doi:10.7717/peerj.5661

648 Singer, R., Araujo, I., Ivory, M.H., 1983. The ectotrophically mycorrhizal fungi of the

649 neotropical lowlands, especially central Amazonia.(Litter decomposition and

650 ectomycorrhiza in Amazonian forests 2.). *Beihefte Zur Nova Hedwigia*.

651 Sombroek, W., 2000. Amazon landforms and soils in relation to biological diversity. *Acta*

652 *Amazonica* 30, 81.

653 Tang, Y., Horikoshi, M., Li, W., 2016. ggfortify: unified interface to visualize statistical results

654 of popular R packages. *R J.* 8, 474.

655 Team, Q.D., 2015. QGIS geographic information system. Open Source Geospatial Foundation

656 Project, Versão 2.

657 Team, Rs., 2015. RStudio: integrated development for R. RStudio, Inc., Boston, MA URL

658 [Http://Www. Rstudio. Com](http://www.Rstudio.com) 42, 84.

659 Tedersoo, L., Bahram, M., Põlme, S., Kõljalg, U., Yorou, N.S., Wijesundera, R., Ruiz, L.V.,

660 Vasco-Palacios, A.M., Thu, P.Q., Suija, A., Smith, M.E., Sharp, C., Saluveer, E., Saitta, A.,  
661 Rosas, M., Riit, T., Ratkowsky, D., Pritsch, K., Pöldmaa, K., Piepenbring, M., Phosri, C.,  
662 Peterson, M., Parts, K., Pärtel, K., Otsing, E., Nouhra, E., Njouonkou, A.L., Nilsson, R.H.,  
663 Morgado, L.N., Mayor, J., May, T.W., Majuakim, L., Lodge, D.J., Lee, S.S., Larsson, K.-  
664 H., Kohout, P., Hosaka, K., Hiiesalu, I., Henkel, T.W., Harend, H., Guo, L., Greslebin, A.,  
665 Grelet, G., Geml, J., Gates, G., Dunstan, W., Dunk, C., Drenkhan, R., Dearnaley, J., De  
666 Kesel, A., Dang, T., Chen, X., Buegger, F., Brearley, F.Q., Bonito, G., Anslan, S., Abell, S.,  
667 Abarenkov, K., 2014. Global diversity and geography of soil fungi. *Science* (New York,  
668 N.Y.) 346, 1052–3. doi:10.1126/science.aaa1185

669 ter Steege, H., Hammond, D.S., 2001. Character convergence, diversity, and disturbance in  
670 tropical rain forest in Guyana. *Ecology* 82, 3197–3212.

671 Van Rossum, G., Drake, F.L., 2009. *Python 3 References Manual*. Scotts Valley CA:  
672 CreateSpace.

673 Wickham, H., 2017. *tidyverse: Easily Install and Load “Tidyverse” Packages* (Version R  
674 package version 1.1. 1).

675 Wickham, H., 2016. *ggplot2: elegant graphics for data analysis*. Springer.

676 Wittmann, F., Schöngart, J., Junk, W.J., 2010. Phytogeography, species diversity, community  
677 structure and dynamics of central Amazonian floodplain forests, in: *Amazonian Floodplain*  
678 *Forests*. Springer, pp. 61–102.

679 Zinger, L., Taberlet, P., Schimann, H., Bonin, A., Boyer, F., De Barba, M., Gaucher, P., Gielly,  
680 L., Giguët-Covex, C., Iribar, A., Réjou-Méchain, M., Rayé, G., Rioux, D., Schilling, V.,

681 Tymen, B., Viers, J., Zouiten, C., Thuiller, W., Coissac, E., Chave, J., 2019. Body size  
682 determines soil community assembly in a tropical forest. *Molecular Ecology* 28, 528–543.  
683 doi:10.1111/mec.14919

684

685

686 Tables:

687

688 **Table 1.** Variables used in model selection with their respective delta dAICc and weight values.

689 The best fit model has a dAICc = 0 and is presented in bold as the alternative good models

690 (dAICc =< 2). The response variables are below-ground Fisher's diversity for prokaryotes (16S)

691 and eukaryotes (18S). The independent variables are flood level, sample type, water mark

692 (measured floodwater marks on trees, with terra firme being zero), and the woody plant Fisher's

693 diversity. The model used flood level and sample type as a fixed factor or as interacting variable.

Marker	Model	AICc	dAICc	df	weight
Prokaryote (16S)	~ 1	89	15.9	2	<0.001
	~ Flood level	96.5	23.4	5	<0.001
	~ Sample type	75.5	2.3	3	0.2355
	~ Water mark	89.7	16.5	3	<0.001
	~ PC1	91.9	18.7	3	<0.001
	~ PC1 * Flood level	127.2	54	9	<0.001
	~ Fisher div.	85.6	12.5	3	0.0015
	~ Fisher div. * Flood level	113.3	40.1	9	<0.001
	~ <b>Fisher div. * Sample</b>	<b>73.1</b>	<b>0</b>	<b>5</b>	<b>0.7625</b>
Eukaryote (18S)	~ 1	86.2	3.8	2	0.066
	~ Flood level	94	11.6	5	0.0013
	~ <b>Sample type</b>	<b>82.4</b>	<b>0</b>	<b>3</b>	<b>0.4357</b>
	~ Watermark	89.2	6.8	3	0.0148
	~ PC1	91.9	9.4	3	0.0039
	~ PC1 * Flood level	127.2	44.7	9	<0.001

~ <b>Fisher div.</b>	<b>83.6</b>	<b>1.1</b>	<b>3</b>	<b>0.2454</b>
~ Fisher div. * Flood level	111.7	29.3	9	<0.001
~ <b>Fisher div. * Sample</b>	<b>83.7</b>	<b>1.3</b>	<b>5</b>	<b>0.2328</b>

---

694

695

696

697 **Table 2.** Estimated parameters (values estimated with standardize error, t-value and respective p-  
 698 value) of the best fit model for 16S and the third best fit model (that included the variables  
 699 selected) for 18S selected in model selection. The response variables are below-ground Fisher's  
 700 alpha diversity and (above-ground) woody plant Fisher's alpha diversity with an interaction term  
 701 between the above-ground alpha diversity and sample type (soil or litter). Significant factors ( $p <$   
 702 0.05) are marked in bold.

	<b>Coefficients</b>	<b>Estimate</b>	<b>Std. Error</b>	<b>t value</b>	<b>Pr(&gt; t )</b>
<b>Prokaryote (16S)</b>	(Intercept)	0.6427	0.1815	3.54	0.00167
	fisher.alpha	-0.2288	0.1947	-1.175	0.2515
	<b>SampleSoil</b>	<b>-1.3463</b>	<b>0.2774</b>	<b>-4.853</b>	<b>6.03E-05</b>
	fisher.alpha:SampleSoil	0.4439	0.2797	1.587	0.12566
<b>Eukaryote (18S)</b>	(Intercept)	0.43232	0.23733	1.822	0.0816
	fisher.alpha	-0.03453	0.25159	-0.137	0.892
	<b>SampleSoil</b>	<b>-0.89964</b>	<b>0.35607</b>	<b>-2.527</b>	<b>0.0189</b>
	fisher.alpha:SampleSoil	0.43738	0.36073	1.212	0.2376

703

704